

Estimating the potential of SWGO to measure the composition-dependent behaviour of the CR anisotropy

Rodrigo Guedes Lang,^{a,*} Paolo Desiati,^b Gwenael Giacinti,^c Samridha Kunwar^d and Andrew M. Taylor^e for the SWGO collaboration

^a*Friedrich-Alexander-Universität Erlangen-Nürnberg, Erlangen Centre for Astroparticle Physics, Nikolaus-Fiebiger-Str. 2, D 91058 Erlangen, Germany*

^b*Department of Physics, University of Wisconsin-Madison, Madison, WI, USA*

^c*Tsung-Dao Lee Institute & School of Physics and Astronomy, Shanghai Jiao Tong University, 520 Shengrong Road, Shanghai 201210, China*

^d*Max-Planck-Institut für Kernphysik, Saupfercheckweg 1, 69117 Heidelberg, Germany*

^e*DESY, D-15738 Zeuthen, Germany*

E-mail: rodrigo.lang@fau.de

Current cosmic ray anisotropy experiments have shown a significant swing in both the direction and the amplitude of the dipole at energies around tens of TeV. Due to the charged nature of these particles, and the presence of magnetic fields in our galaxy, an underlying composition-dependent dipole swing is expected. For this reason, combining measurements of the composition and the distribution of arrival directions is essential for unveiling the astrophysical origin of this structure. In this work, we study the potential of the upcoming Southern Wide-field Gamma-ray Observatory (SWGO) in contributing to these anisotropy studies. We present a template-based method developed for reconstructing the number of muons and separating primary cosmic rays. Preliminary resolutions of 5 – 30% in the number of muons and an accuracy of 70 – 90% in the species separation are found. A clear improvement is seen by considering a dedicated muon-counter layer in a detector, highlighting the future potential of SWGO.

38th International Cosmic Ray Conference (ICRC2023)
26 July - 3 August, 2023
Nagoya, Japan



*Speaker

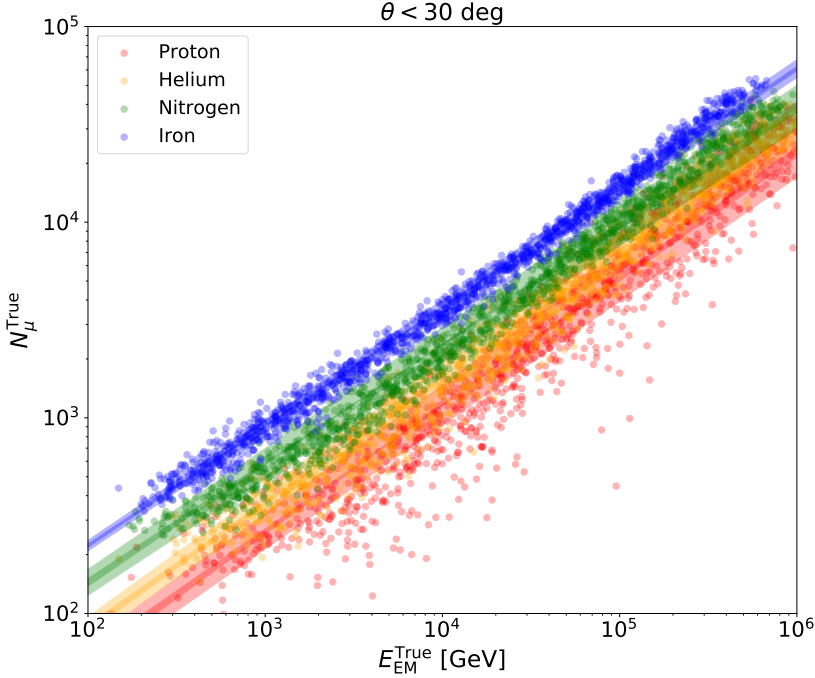


Figure 1: True number of muons at the detector level versus true electromagnetic energy for different primaries. The shaded regions show the result of a linear fit in $\log_{10} N_{\mu}^{\text{true}}$ and $\log_{10} N_{\text{EM}}^{\text{true}}$.

1. Introduction

One of the main tools for investigating the origin of cosmic rays is the study of the anisotropy in their distribution of arrival directions. As expected from their charged nature, these particles arrive strongly isotropically. Nevertheless, advances in experimental techniques and accumulation of the large exposures from cosmic ray experiments have allowed the probing of the levels of the dipole and higher multipoles of the distribution.

Currently, a dipole amplitude of $\sim 10^{-3}$ is measured up to tens of TeV, at which a significant swing in the dipole phase is seen accompanied by a corresponding drop in the amplitude [1]. The origin of this effect is yet to be understood. However, due to the magnetic origin of the acceleration of these particles, a composition-dependent effect is naturally expected. No current mass-dependent anisotropy data is available to test this hypothesis and, thus, future measurements as such are desirable.

Separating between primaries using ground-based cosmic ray detectors, such as the experiments designed for this energy range, has proven a hard task due to the stochastic nature of the air showers generated by these particles in the atmosphere. Nevertheless, good separation could be obtained if information about secondary muons could be accessed [2]. Figure 1 shows the expected number of muons at the detector level versus the electromagnetic energy of the air shower for example simulations of different cosmic ray primaries. A decent separation is found for at least four primaries (proton, helium, nitrogen, and iron). The heavier the mass, the smaller the spread,

as expected from the superposition model. Therefore, future experiments with muon-counting capabilities could improve our understanding of the origin of cosmic rays.

The current generation of ground-based water Cherenkov gamma-ray detectors is well established, leading to important results in the field [3, 4]. The Southern Wide-field Gamma-ray Observatory (SWGO) is a future ground-based wide-field gamma-ray and cosmic-ray detector in the research and development stage to be built in South America, expanding the current generation of experiments to the Southern Hemisphere [5]. One of the considered detector designs consists of a dual-layered water Cherenkov tank. Electromagnetic secondary particles of the shower are expected to deposit their energy calorimetrically in the top chamber of the tank. Muons, on the other hand, are expected to pass through both chambers, emitting light proportionally to their traveled distance. For that reason, a dual-layered design provides a crucial tool for muon counting and, thus, SWGO could contribute to further cosmic ray anisotropy studies.

In this work, we develop a template-based method for reconstructing the number of muons of TeV-PeV cosmic ray air showers as well as separating between primary species, which is presented in Section 2. The method is then used to calculate preliminary estimations of the capabilities of SWGO in such studies, whose results are shown in Section 3. Finally, conclusions and future steps are addressed in Section 4.

2. Template method

Template-based methods have been proven as efficient tools for the reconstruction of gamma-ray showers with ground-based detectors [6]. It is based on building up probability density functions (PDF) for physical quantities measured by the experiments in bins for the quantities to be reconstructed and further comparing measured events to these PDFs.

For the proof of concept here presented, we used a small preliminary set of simulations. Four input primaries (P, He, N, and Fe) were considered and, for each, 5000 events were simulated using the CORSIKA (version 7.7410) [7] and GEANT4 (version geant4-10-00-patch-04) [8] simulation packages. The used hadronic interaction models for low and high energies were, respectively, UrQMD 1.3.1 [9, 10] and QGSJET-II-04 [11]. The energy spectrum was taken as E^{-1} from 10^1 TeV to $10^{3.5}$ TeV so that each template would have roughly the same statistics. Zenith angles between 0° and 65° equally distributed in $\sin^2 \theta$ were chosen. Only showers falling inside the array were simulated. One of the proposed detector designs and layouts is considered, consisting of 3.82 m wide and 3 m tall water tanks, divided into two layers with 2.5 m (top) and 0.5 m (bottom). The layout consists of two zones: the inner array with 5731 tanks in a circle of 160 m radius, resulting in a fill factor of 80%, and the outer array with 858 tanks in a circle of 300 m radius, resulting in a fill factor of 5%.

Templates were binned in bins of true zenith angle, θ , true number of muons at the detector level, N_μ^{true} , and true primary species. For the proof of concept, only one zenith bin, $(0, 30)^\circ$, was considered and N_μ^{true} bins were divided into 10 bins per decade. Two different sets of templates were built by filling 2D or 3D histograms with the individual tank information for each event that fits the bin criteria. For the 2D templates, the charge measured on the top chamber of the tank, q_{top} , and the distance of the tank to the true shower core on the shower plane¹ were used. The 3D templates add

¹This compensates for the effects coming from different zenith angles and allows for a broader zenith binning.

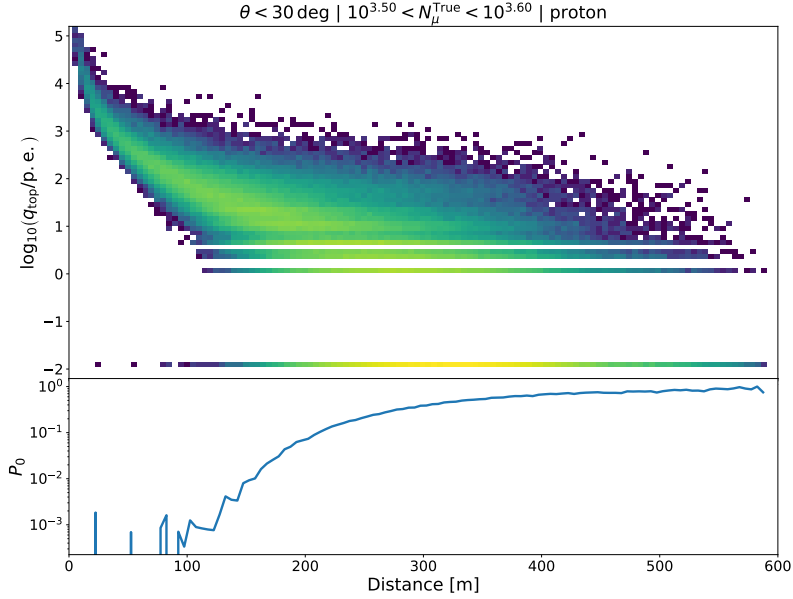


Figure 2: Example 2D template for true proton events with $\theta < 30$ deg and $10^{3.5} < N_\mu^{\text{true}} < 10^{3.6}$. Each entry in the 2D histogram is the information of an individual tank in an event. The x axis represents the distance of the tank to the true shower core position on the shower plane, while the y axis represents the simulated charge measured on the top chamber of the tank. Tanks that didn't measure any charge are stored at $\log_{10}(q_{\text{top}}/\text{p.e.}) = -2$, resulting in the bottom horizontal line. This line is broken down in the bottom panel, which shows the probability of a tank at a given distance detecting no signal.

POS (ICRC2023) 486

a new dimension by considering the charge measured in the lower chamber, q_{bot} . Figure 2 shows an example 2D template. The lateral distribution function (LDF) of an average shower that fits the bin criteria can clearly be seen in the pdf. The 3D templates have a similar structure.

Once the templates are built, events can be reconstructed by comparing their tank information distribution to the pdfs. The likelihood of an event being described by the pdf of each template bin is calculated. The likelihood profile for an example event is shown in Figure 3. For each primary and given dimension template, the profile shows a well-defined minimum. Events reconstructed using templates of heavier masses (blue line in the example plot) will likely overestimate the number of muons, while events reconstructed using templates of lighter masses (red and orange lines in the example plot) will likely underestimate it. Nevertheless, no prior can be done about the true primary species and, thus, a specific likelihood profile cannot be chosen. The reconstructed number of muons is, thus, taken as the one with the lowest likelihood value between the four minima (green in the example plot). In the same way, the reconstructed primary is taken as the primary for which the likelihood value was the lowest (nitrogen in the example plot). 2D and 3D reconstructions are done independently.

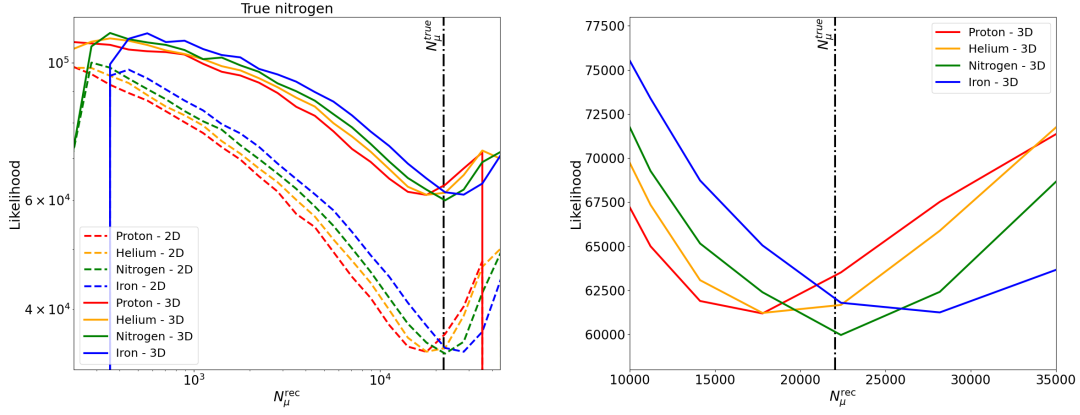


Figure 3: Likelihood profile as a function of the reconstructed number of muons for an example event. Different colors represent different true primary templates. Dashed and full lines represent results using 2D and 3D templates respectively. The dashed black line shows the true number of muons for this event. The right-hand side panel shows a zoom in the region around the minimum likelihood.

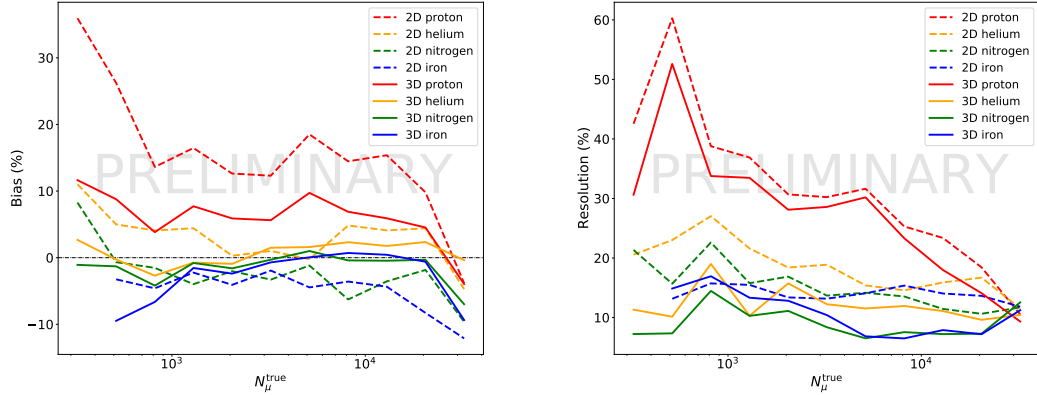


Figure 4: Bias (left) and resolution (right) of the reconstructed number of muons. Different colors represent different true primaries. Dashed and full lines represent results using 2D and 3D templates respectively. The bias and resolution are defined as the mean and RMS of the $(N_\mu^{\text{rec}} - N_\mu^{\text{true}})/N_\mu^{\text{true}}$ distribution.

3. Results

Following this procedure, the number of muons and primary species for the events in the simulation set were reconstructed. The bias and resolution in the number of muons were calculated as the mean and RMS of the $(N_\mu^{\text{rec}} - N_\mu^{\text{true}})/N_\mu^{\text{true}}$ distribution and are shown in Figure 4. As expected due to the spread shown in Figure 1, the reconstruction of protons achieves the worst results, while the best results are obtained for heavier masses, such as nitrogen and iron. A clear improvement in the reconstruction is seen by adding the information of the bottom chamber, i.e., going from a 2D to a 3D reconstruction.

The accuracy in the particle species separation is shown in Figure 5. Once more, a clear

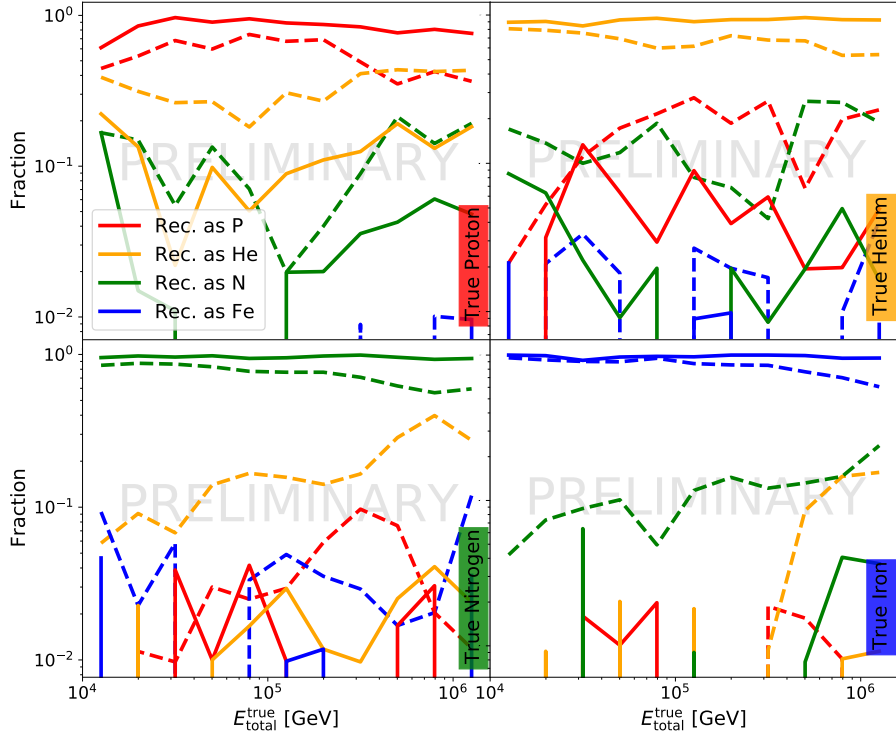


Figure 5: Reconstructed primary as a function of true energy for different test primaries. Different colors represent different reconstructed primaries. Dashed and full lines represent results using 2D and 3D templates respectively. Each panel represents a different true test primary (in order: proton, helium, nitrogen, and iron).

improvement is seen by using the 3D templates, leading to 70 – 90% correctly reconstructed species depending on the true primary and energy.

4. Conclusions

In this work, we have proposed a template-based method for the reconstruction of the number of muons and primary species separation of cosmic ray air showers for the upcoming SWGO experiment. A proof of concept of the method was shown by applying it to a small set of preliminary simulations. Preliminary results are in line with expectations, validating the method. Strong improvements in both the reconstruction and the separation were seen by adding the information of the bottom chamber of a dual-layered water Cherenkov tank, highlighting the potential of SWGO in performing such measurements. Further investigations are planned, e.g., by having larger statistics, wider energy and zenith angle ranges and improving the procedure for the template building.

References

- [1] A. U. Abeysekara *et al.* [HAWC and IceCube], “All-Sky Measurement of the Anisotropy of Cosmic Rays at 10 TeV and Mapping of the Local Interstellar Magnetic Field,” *Astrophys. J.* **871** (2019) no.1, 96 doi:10.3847/1538-4357/aaf5cc [arXiv:1812.05682 [astro-ph.HE]].
- [2] A. M. Taylor *et al.* [SWGO], “Composition Sensitivity for the Cosmic Ray Anisotropy with SWGO,” PoS **ICRC2021** (2021), 198 doi:10.22323/1.395.0198 [arXiv:2108.04609 [astro-ph.HE]].
- [3] A. U. Abeysekara *et al.* “Observation of the Crab Nebula with the HAWC Gamma-Ray Observatory,” *Astrophys. J.* **843** (2017) no.1, 39 doi:10.3847/1538-4357/aa7555 [arXiv:1701.01778 [astro-ph.HE]].
- [4] G. Di Sciascio [LHAASO], “The LHAASO experiment: from Gamma-Ray Astronomy to Cosmic Rays,” *Nucl. Part. Phys. Proc.* **279-281** (2016), 166-173 doi:10.1016/j.nuclphysbps.2016.10.024 [arXiv:1602.07600 [astro-ph.HE]].
- [5] A. Albert *et al.* “Science Case for a Wide Field-of-View Very-High-Energy Gamma-Ray Observatory in the Southern Hemisphere,” [arXiv:1902.08429 [astro-ph.HE]].
- [6] V. Joshi, J. Hinton, H. Schoorlemmer, R. López-Coto and R. Parsons, “A template-based γ -ray reconstruction method for air shower arrays,” *JCAP* **01** (2019), 012 doi:10.1088/1475-7516/2019/01/012 [arXiv:1809.07227 [astro-ph.IM]].
- [7] D. Heck, J. Knapp, J. N. Capdevielle, G. Schatz and T. Thouw, “CORSIKA: A Monte Carlo code to simulate extensive air showers,” FZKA-6019.
- [8] S. Agostinelli *et al.* [GEANT4], “GEANT4—a simulation toolkit,” *Nucl. Instrum. Meth. A* **506** (2003), 250-303 doi:10.1016/S0168-9002(03)01368-8
- [9] S. A. Bass, M. Belkacem, M. Bleicher, M. Brandstetter, L. Bravina, C. Ernst, L. Gerland, M. Hofmann, S. Hofmann and J. Konopka, *et al.* “Microscopic models for ultrarelativistic heavy ion collisions,” *Prog. Part. Nucl. Phys.* **41** (1998), 255-369 doi:10.1016/S0146-6410(98)00058-1 [arXiv:nucl-th/9803035 [nucl-th]].
- [10] M. Bleicher, E. Zabrodin, C. Spieles, S. A. Bass, C. Ernst, S. Soff, L. Bravina, M. Belkacem, H. Weber and H. Stoecker, *et al.* *J. Phys. G* **25** (1999), 1859-1896 doi:10.1088/0954-3899/25/9/308 [arXiv:hep-ph/9909407 [hep-ph]].
- [11] S. Ostapchenko, “Monte Carlo treatment of hadronic interactions in enhanced Pomeron scheme: I. QGSJET-II model,” *Phys. Rev. D* **83** (2011), 014018 doi:10.1103/PhysRevD.83.014018 [arXiv:1010.1869 [hep-ph]].

The SWGO Collaboration



P. Abreu^{1,2}, A. Albert³, R. Alfaro⁴, A. Alfonso⁵, C. Álvarez⁶, Q. An⁷, E. O. Angüner⁸, C. Arcaro⁹, R. Arceo⁶, S. Arias¹⁰, H. Arnaldi¹¹, P. Assis^{1,2}, H. A. Ayala Solares¹², A. Bakalova¹³, U. Barres de Almeida^{14,15}, I. Batkovic^{9,16}, J. Bazo¹⁷, J. Bellido^{18,19}, E. Belmont⁴, S. Y. BenZvi²⁰, A. Bernal²¹, W. Bian²², C. Bigongiari²³, E. Bottacini^{9,16}, P. Brogueira^{1,2}, T. Bulik²⁴, G. Busetto^{9,16}, K. S. Caballero-Mora⁶, P. Camarri^{25,26}, S. Campos²⁷, W. Cao⁷, Z. Cao⁷, Z. Cao²⁸, T. Capistrán²¹, M. Cardillo²³, E. Carquin²⁹, A. Carramíñana³⁰, C. Castromonte³¹, J. Chang²⁸, O. Chaparro³², S. Chen²², M. Chianese^{33,34}, A. Chiavassa^{35,36}, L. Chytka¹³, R. Colallillo^{33,34}, R. Conceição^{1,2}, G. Consolati^{37,38}, R. Cordero³⁹, P. J. Costa^{1,2}, J. Cotzomi⁴⁰, S. Dasso⁴¹, A. De Angelis^{9,16}, P. Desiati⁴², F. Di Pierro³⁶, G. Di Sciascio²⁵, J. C. Díaz Vélez⁴², C. Dib²⁹, B. Dingus³, J. Djupsland⁴³, C. Dobrigkeit⁴⁴, L. M. Domingues Mendes^{1,45}, T. Dorigo⁹, M. Doro^{9,16}, A. C. dos Reis¹⁴, M. Du Vernois⁴², M. Echiburú⁵, D. Elsaesser⁴⁶, K. Engel^{2,47}, T. Ergin⁴⁸, F. Espinoza⁵, K. Fang⁴², F. Farfán Carreras⁴⁹, A. Fazzi^{38,50}, C. Feng⁵¹, M. Feroci²³, N. Fraija²¹, S. Fraija²¹, A. Franceschini¹⁶, G. F. Franco¹⁴, S. Funk⁵², S. García¹⁰, J. A. García-González⁵³, F. Garfias²¹, G. Giacinti²², L. Gibilisco^{1,2}, J. Glombitzka⁵², H. Goksu⁴³, G. Gong⁵⁴, B. S. González^{1,2}, M. M. Gonzalez²¹, J. Goodman⁴⁷, M. Gu²⁸, F. Guarino^{33,34}, S. Gupta⁵⁵, F. Haist⁴³, H. Hakobyan²⁹, G. Han⁵⁶, P. Hansen⁵⁷, J. P. Harding³, J. Helo⁵, I. Herzog⁵⁸, H. d. Hidalgo⁶, J. Hinton⁴³, K. Hu⁵¹, D. Huang⁴⁷, P. Huentemeyer⁵⁹, F. Hueyotl-Zahuantitla⁶, A. Iriarte²¹, J. Isaković⁶⁰, A. Isolia⁶¹, V. Joshi⁵², J. Juryšek¹³, S. Kaci²², D. Kieda⁶², F. La Monaca²³, G. La Mura¹, R. G. Lang⁵², R. Laspiur²⁷, L. Lavitolá³⁴, J. Lee⁶³, F. Leitl⁵², L. Lessio²³, C. Li²⁸, J. Li⁷, K. Li²⁸, T. Li²², B. Liberti^{25,26}, S. Lin⁶⁴, D. Liu⁵¹, J. Liu²⁸, R. Liu⁶⁵, F. Longo^{66,67}, Y. Luo²², J. Lv⁶⁸, E. Macerata^{38,50}, K. Malone³, D. Mandat¹³, M. Manganaro⁶⁰, M. Mariani^{38,50}, A. Mariazzi⁵⁷, M. Mariotti^{9,16}, T. Marrodan⁴³, J. Martínez³², H. Martínez-Huerta⁶⁹, S. Medina⁵, D. Melo⁷⁰, L. F. Mendes², E. Meza⁷², D. Miceli⁹, S. Miozzo²⁵, A. Mitchell⁵², A. Molinario^{36,71}, O. G. Morales-Olivares⁶, E. Moreno⁴⁰, A. Morselli^{25,26}, E. Mossini^{38,50}, M. Mostafá¹², F. Muleri²³, F. Nardi^{9,16}, A. Negro^{35,36}, L. Nellen⁷³, V. Novotny¹³, E. Orlando^{66,67}, M. Osorio²¹, L. Otiniano⁷², M. Peresano^{35,36}, G. Piano²³, A. Pichel⁴¹, M. Pihet^{9,16}, M. Pimenta^{1,2}, E. Prandini^{9,16}, J. Qin⁷, E. Quispe^{72,74}, S. Rainò⁷⁵, E. Rangel²¹, A. Reisenegger⁵⁵, H. Ren⁴³, F. Reščić⁶⁰, B. Reville⁴³, C. D. Rho⁷⁶, M. Riquelme⁷⁷, G. Rodriguez Fernandez²⁵, Y. Roh⁶³, G. E. Romero⁴⁹, B. Rossi³⁴, A. C. Rovero⁴¹, E. Ruiz-Velasco⁴³, G. Salazar²⁷, J. Samanes⁷², F. Sanchez⁷⁰, A. Sandoval⁴, M. Santander⁷⁸, R. Santonico^{25,26}, G. L. P. Santos¹⁴, N. Saviano^{33,34}, M. Schneider⁴⁷, M. Schneider⁵², H. Schoorlemmer⁷⁹, J. Serna-Franco⁴, V. Serrano²⁷, A. Smith⁴⁷, Y. Son⁶³, O. Soto⁸⁰, R. W. Springer⁶², L. A. Stuani⁸¹, H. Sun⁵¹, R. Tang²², Z. Tang⁷, S. Tapia²⁹, M. Tavani²³, T. Terzić⁶⁰, K. Tollefson⁵⁸, B. Tomé^{1,2}, I. Torres³⁰, R. Torres-Escobedo²², G. C. Trinchero^{36,71}, R. Turner⁵⁹, P. Ulloa⁸⁰, L. Valore^{33,34}, C. van Eldik⁵², I. Vergara⁵⁷, A. Viana⁸², J. Víchá¹³, C. F. Vigorito^{35,36}, V. Vittorini²³, B. Wang⁵¹, J. Wang⁴³, L. Wang²⁸, X. Wang⁵⁹, X. Wang⁶⁵, X. Wang⁸³, Z. Wang²², M. Waqas^{33,34}, I. J. Watson⁶³, F. Werner⁴³, R. White⁴³, C. Wiebusch⁸⁴, E. J. Wilcox⁴⁷, F. Wohlleben⁴³, S. Wu²⁸, S. Xi²⁸, G. Xiao²⁸, L. Yang⁶⁴, R. Yang⁷, R. Yanyachi¹⁸, Z. Yao²⁸, D. Zavrtanik⁸⁵, H. Zhang²², H. Zhang⁶⁵, S. Zhang⁸⁶, X. Zhang²⁸, Y. Zhang⁶⁸, J. Zhao²⁸, L. Zhao⁷, H. Zhou²², C. Zhu⁵¹, P. Zhu⁸⁶, X. Zuo²⁸

¹ Laboratório de Instrumentação e Física Experimental de Partículas - LIP, Av. Prof. Gama Pinto, 2, 1649-003 Lisboa, Portugal

² Departamento de Física, Instituto Superior Técnico, Universidade de Lisboa, Av. Rovisco Pais 1, 1049-001 Lisboa, Portugal

³ Physics Division, Los Alamos National Laboratory, Los Alamos, NM, USA

⁴ Instituto de Física, Universidad Nacional Autónoma de México, Circuito de la Investigación científica, C.U., A. Postal 70-364, 04510 Cd. de México, México

⁵ Universidad de La Serena, Chile

⁶ Facultad de Ciencias en Física y Matemáticas, Universidad Autónoma de Chiapas, C. P. 29050, Tuxtla Gutiérrez, Chiapas, México

⁷ School of physical science, University of Science and Technology of China, 96 Jinzhai Road, Hefei, Anhui 230026, China

⁸ TÜBİTAK Research Institute for Fundamental Sciences, 41470 Gebze, Turkey

⁹ INFN - Sezione di Padova, I-35131, Padova, Italy

¹⁰ Universidad Nacional de San Antonio Abad del Cusco, Av. de la Cultura, Nro. 733, Cusco - Perú

¹¹ Centro Atómico Bariloche (CNEA-CONICET-IB/UNCuyo), Av. E. Bustillo 9500, (8400) San Carlos de Bariloche, Rio Negro, Argentina

¹² Department of Physics, Pennsylvania State University, University Park, PA, USA

¹³ Institute of Physics of the Czech Academy of Sciences, Prague, Czech Republic

¹⁴ Centro Brasileiro de Pesquisas Físicas (CBPF), Rua Dr. Xavier Sigaud 150, 22290-180 Rio de Janeiro, Brasil

¹⁵ Universidade de São Paulo, Instituto de Astronomia, Geofísica e Ciências Atmosféricas, Departamento de Astronomia, Rua do Matão 1226, 05508-090 São Paulo, Brasil

¹⁶ Università di Padova, I-35131, Padova, Italy

¹⁷ Pontificia Universidad Católica del Perú, Av. Universitaria 1801, San Miguel, 15088, Lima, Perú

¹⁸ Universidad Nacional de San Agustín de Arequipa, Santa Catalina Nro. 117. Arequipa

¹⁹ University of Adelaide, Adelaide, S.A., Australia

²⁰ Department of Physics and Astronomy, University of Rochester, Rochester, NY, USA

²¹ Instituto de Astronomía, Universidad Nacional Autónoma de México, Circuito Exterior, C.U., A. Postal 70-264, 04510 Cd. de México, México

²² Tsung-Dao Lee Institute and School of Physics and Astronomy, Shanghai Jiao Tong University, 520 Shengrong Road, Shanghai 201210, China

- ²³ Istituto Nazionale Di Astrofisica (INAF), Roma, Italy
²⁴ Astronomical Observatory Warsaw University, 00-478 Warsaw, Poland
²⁵ INFN, Roma Tor Vergata, Italy
²⁶ Department of Physics, University of Roma Tor Vergata, Viale della Ricerca Scientifica 1, I-00133 Roma, Italy
²⁷ Facultad de Ciencias Exactas, Universidad Nacional de Salta, Avda. Bolivia 5150, A4408FVY, Salta, Argentina
²⁸ Institute of High Energy Physics, Chinese Academy of Science, 19B Yuquan Road, Shijingshan District, Beijing 100049, China
²⁹ CCTVal, Universidad Técnica Federico Santa María, Chile
³⁰ Instituto Nacional de Astrofísica, Óptica y Electrónica, Puebla, Mexico
³¹ Universidad Nacional de Ingeniería, Av. Túpac Amaru 210 - Rímac. Apartado 1301, Lima Perú
³² Centro de Investigación en Computación, Instituto Politécnico Nacional, Ciudad de México, Mexico
³³ Università di Napoli "Federico II", Dipartimento di Fisica "Ettore Pancini", Napoli, Italy
³⁴ INFN, Sezione di Napoli, Napoli, Italy
³⁵ Università degli Studi di Torino, I-10125 Torino, Italy
³⁶ INFN, Sezione di Torino, Torino, Italy
³⁷ Politecnico di Milano, Dipartimento di Scienze e Tecnologie Aeroespaziali, Milano, Italy
³⁸ INFN, sezione di Milano, Milano, Italy
³⁹ Departamento de Física, Universidad de Santiago de Chile, Chile
⁴⁰ Facultad de Ciencias Físico Matemáticas, Benemérita Universidad Autónoma de Puebla, Av. San Claudio y 18 Sur, Ciudad Universitaria 72570, Puebla, Mexico
⁴¹ Instituto de Astronomía y Física del Espacio (IAFE (CONICET-UBA)), Ciudad Universitaria, CABA, Argentina
⁴² Department of Physics, University of Wisconsin-Madison, Madison, WI, USA
⁴³ Max-Planck-Institut für Kernphysik, Saupfercheckweg 1, 69117 Heidelberg, Germany
⁴⁴ Departamento de Raios Cósmicos e Cronología, Instituto de Física "Gleb Wataghin", Universidade Estadual de Campinas, C.P. 6165, 13083-970 Campinas, Brasil
⁴⁵ Centro Federal de Educação Tecnológica Celso Suckow da Fonseca (CEFET), Rio de Janeiro, Brasil
⁴⁶ Technische Universität Dortmund, D-44221 Dortmund, Germany
⁴⁷ Department of Physics, University of Maryland, College Park, MD, USA
⁴⁸ Middle East Technical University, Northern Cyprus Campus, 99738 Kalkanli via Mersin 10, Turkey
⁴⁹ Instituto Argentino de Radioastronomía (CONICET, CIC, UNLP), Camino Gral. Belgrano Km 40, Berazategui, Argentina
⁵⁰ Politecnico di Milano, Dipartimento di Energia, Milano, Italy
⁵¹ Key Laboratory of Particle Physics and Particle Irradiation (MOE), Institute of Frontier and Interdisciplinary Science, Shandong University, Qingdao, Shandong 266237, China
⁵² Friedrich-Alexander-Universität Erlangen-Nürnberg, Erlangen Centre for Astroparticle Physics, Nikolaus-Fiebiger-Str. 2, D 91058 Erlangen, Germany
⁵³ Tecnológico de Monterrey, Escuela de Ingeniería y Ciencias, Ave. Eugenio Garza Sada 2501, Monterrey, N.L., Mexico, 64849
⁵⁴ Dept. of Engineering Physics, Tsinghua University, 1 Tsinghua Yuan, Haidian District, Beijing 100084, China
⁵⁵ Universidad Metropolitana de Ciencias de la Educación (UMCE), Chile
⁵⁶ School of Mechanical Engineering and Electronic Information, China University of Geosciences, Wuhan, Hubei 430074, China
⁵⁷ IFLP, Universidad Nacional de La Plata and CONICET, La Plata, Argentina
⁵⁸ Department of Physics and Astronomy, Michigan State University, East Lansing, MI, USA
⁵⁹ Michigan Technological University, Houghton, Michigan, 49931, USA
⁶⁰ University of Rijeka, Faculty of Physics, 51000 Rijeka, Croatia
⁶¹ Università di Catania, Catania, Italy
⁶² Department of Physics and Astronomy, University of Utah, Salt Lake City, UT, USA
⁶³ University of Seoul, Seoul, Rep. of Korea
⁶⁴ School of Physics and Astronomy, Sun Yat-sen University, Zhuhai, Guangdong 519082, China
⁶⁵ School of Astronomy and Space Science, Nanjing University, Xianlin Avenue 163, Qixia District, Nanjing, Jiangsu 210023, China
⁶⁶ Dipartimento di Fisica, Università degli Studi di Trieste, Trieste, Italy
⁶⁷ INFN - Sezione di Trieste, via Valerio 2, I - 34149, Trieste, Italy
⁶⁸ Aerospace Information Research Institute, Chinese Academy of Science, 9 Dengzhuang South Road, Haidian District, Beijing 100094, China
⁶⁹ Departamento de Física y Matemáticas, Universidad de Monterrey, Av. Morones Prieto 4500, 66238, San Pedro Garza García NL, México
⁷⁰ Instituto de Tecnologías en Detección y Astropartículas (CNEA, CONICET, UNSAM), Buenos Aires, Argentina
⁷¹ Instituto Nazionale Di Astrofisica (INAF), Torino, Italy
⁷² Comisión Nacional de Investigación y Desarrollo Aeroespacial, Perú
⁷³ Instituto de Ciencias Nucleares, Universidad Nacional Autónoma de México, Circuito Exterior, C.U., A. Postal 70-543, 04510 Cd. de México, México
⁷⁴ Universidad Nacional de Moquegua, None
⁷⁵ Università degli Studi di Bari Aldo Moro, Italy
⁷⁶ Department of Physics, Sungkyunkwan University, Suwon, South Korea

⁷⁷ Universidad de Chile, Chile

⁷⁸ Department of Physics and Astronomy, University of Alabama, Tuscaloosa, Alabama, 35487, USA

⁷⁹ IMAPP, Radboud University Nijmegen, Nijmegen, The Netherlands

⁸⁰ Unidade Acadêmica de Física, Universidade Federal de Campina Grande, Av. Aprígio Veloso 882, CY2, 58.429-900 Campina Grande, Brasil

⁸¹ Instituto de Física de São Carlos, Universidade de São Paulo, Av. Trabalhador São-carlense 400, São Carlos, Brasil

⁸² School of Integrated Circuit, Ludong University, 186 Hongqi Middle Road, Zhifu District, Yantai, Shandong, China

⁸³ III. Physics Institute A, RWTH Aachen University, Templergraben 56, D-52062 Aachen, Germany

⁸⁴ Center for Astrophysics and Cosmology (CAC), University of Nova Gorica, Nova Gorica, Slovenia

⁸⁵ College of Engineering, Hebei Normal University, 20 South Second Ring East Road, Shijiazhuang, Hebei, China

⁸⁶ School of mechanical engineering, University of Science and Technology Beijing, 30 Xueyuan Road, Haidian District, Beijing 100083, China